

On the nature of the X-ray source 1E 1024.0–5732/Wack 2134

Pablo Reig^{1,2,3}

¹ Physics and Astronomy Department, Southampton University, Southampton, SO17 1BJ, UK

² Foundation for Research and Technology-Hellas, GR-71110 Heraklion, Crete, Greece

³ Physics Department, University of Crete, GR-71003 Heraklion, Crete, Greece

Received 27 November 1998 / Accepted 1 March 1999

Abstract. Two different models have been put forward to explain the origin of the X-ray emission of the unusual X-ray source 1E 1024.0–5732/Wack 2134: a high-mass X-ray binary system (HMXB) and a colliding wind binary (CWB). We present new optical and X-ray data in an attempt to clarify the nature of this system. The data seem to favour the colliding wind model since the optical spectra show characteristics of both, a Wolf-Rayet and an O-type star, implying that these two type of stars may be present in the system. The lack of coherent modulation (pulsations) and the relatively soft and low luminosity X-ray emission seems to exclude the presence of a neutron star as the body generating the X-ray emission. We present the first X-ray energy spectrum of this source at energies above 3 keV and discuss the implications of the spectral parameters obtained from the model fitting. We comment on the fact that the iron lines in CWB are centred at higher energies, ~ 6.6 keV, than those detected in supergiant HMXB, where a value of 6.4 keV is found, implying that the degree of ionisation of iron is higher in CWB.

Key words: stars: individual: 1 E 1024-5232 = Wack 2134 – stars: Wolf-Rayet – X-rays: stars

1. Introduction

The source 1E 1024.0–5732 was discovered serendipitously with the *Einstein Observatory* by Goldwurm et al. (1987) when they were searching for soft X-ray counterparts of the COS B galactic gamma-ray source 2CG 284-00. Caraveo et al. (1989) excluded the possibility that the X-ray emission had a coronal origin on the basis of the ratio between the X-ray and optical flux $f_x/f_{op} \sim 5 \times 10^{-2}$, which would imply an L_x/L_{bol} much larger than the average value of 10^{-7} observed in the first X-ray studies of O-type stars (Cassinelli et al. 1981). The source was visible only in seven Einstein IPC energy channels (0.5–3.5 keV), making any spectral fitting procedure very uncertain. The data fitted equally well to a power-law, bremsstrahlung and blackbody models and therefore the X-ray spectral parameters were affected by large uncertainties. Caraveo et al. (1989) also

reported a periodicity of 60.69272 ± 0.00006 seconds, which they attributed to the rapid spin of a compact companion. From their optical observations they concluded that Wackerling 2134, a highly reddened O5 star at an estimated maximum distance of 3 kpc was the most likely optical counterpart. Therefore the scenario proposed by these authors to explain the nature of 1E 1024.0–5732 was that of a massive X-ray binary in which a hot O5 type star loses mass to a spinning neutron star. The X-ray emission would be due to the accretion mechanism via the strong stellar wind of the optical primary.

Mereghetti et al. (1994) confirmed the association of the X-ray source 1E 1024.0–5732 with Wack 2134. However, using data from a ROSAT PSPC observation they failed to detect any periodic modulation. The lack of pulsations and the dependence of L_x/L_{bol} on the poorly constrained interstellar absorption led these authors to prefer the interpretation of this source as a binary system consisting of a Wolf-Rayet primary and an O-type star secondary. In this case, the X-ray emission would be produced as a consequence of the collision of their very strong stellar winds.

2. Observations and data reduction

2.1. Optical spectra

We obtained three optical spectra of Wack 2134 on June 20, 21 and 23, 1997 using the 1.9m telescope at the South African Astronomical Observatory (SAAO). All three spectra were taken with the ITS spectrograph and the SITe CCD detector. The 1200 $l\text{ mm}^{-1}$ grating No 5, blazed at 6800 Å, was used in first order on the night June 20, 1997, whereas the 1200 $l\text{ mm}^{-1}$ grating No 4, blazed at 4600 Å, also in first order, was used on the other two nights. The slit width was set to 250 μm . With this set-up the dispersion was ~ 0.5 Å/pixel.

Table 1 gives the journal of the optical spectroscopic observations. The data were reduced using the *Starlink* supported FIGARO package (Shortridge et al. 1997).

2.2. X-ray data

1E 1024.0–5732 was observed with the *Proportional Counter Array* (PCA) (Jahoda et al. 1996) onboard the *Rossi X-ray Timing Explorer* (RXTE) on November 29, 1997 for a total on-

Table 1. The journal of the optical spectroscopic observations

Julian Date (2,400,000+)	Date	Wavelength range (Å)	He II $\lambda 6563/H\alpha$			He II $\lambda 4686$		
			EW	FWHM	Centre	EW	FWHM	Centre
50620	20JUN97	6180–6900	–22.2	45.4	6568.3			
50621	21JUN97	3970–4850				–6.8	20	4690.5
50623	23JUN97	3970–4850				–6.8	20	4689.7

EW, FWHM and centre are given in Å.

FWHM not corrected for instrumental broadening.

Errors are $\sim 10\%$.

source time of 25 ksec. Data reduction was carried out using the specific package for RXTE in *ftools*, whereas data analysis was done using version 10 of the XSPEC X-ray spectral modeling software (Arnaud 1996). In the analysis presented here we used the instrument configuration known as *Good Xenon*, which provides detailed spectra (256 channels) and temporal ($\sim 1 \mu\text{s}$) information about every event that survives background rejection. Good time intervals were defined by removing data taken at low Earth elevation angle ($< 10^\circ$) and during times of high particle background. An offset of only 0.02° between the source position and the pointing of the satellite was allowed, to ensure that any possible short stretch of slew data at the beginning and/or end of the observation was removed. In order to improve the S/N ratio we used only data from the top layer anode of the detectors.

Apart from 1E 1024.0–5732, other X-ray sources may be present in the field of view of the PCA (see Belloni & Mereghetti 1994). Of these, the emission nebula RCW49 is the most prominent. The possible contribution of this second X-ray source was taken into account in the spectral analysis by adding an absorbed bremsstrahlung component with fixed parameters, $N_H = 2 \times 10^{22} \text{ cm}^{-2}$ and $kT = 0.5 \text{ keV}$, as derived from an observation with the *Einstein Observatory* by Goldwurm et al. (1987). This component is not expected to affect appreciably the spectral parameters of the fit since it contributes only at energies below $\sim 3.5 \text{ keV}$, whereas our analysis is done in the energy range 3–15 keV.

3. Results

3.1. Optical spectra

The average of the two blue-end spectra and the red-end spectrum of Wack 2134, the optical counterpart to 1E 1024.0–5732, are shown in Fig. 1. The most salient features are the HeII/H α $\lambda 6563$ and HeII $\lambda 4686$ lines whose equivalent widths (EW), full width at half maximum (FWHM) and line centres are given in Table 1. It is clear from these lines and those of N III (blend) $\lambda 4634$ –40–42 that we are dealing with an Of and/or a nitrogen dominated Wolf-Rayet (WR) star. The following analysis can be done based on the appearance and ratios of the different ions present.

- The presence of hydrogen (H γ , H δ) together with the low abundance of carbon and oxygen rule out the WC classifica-

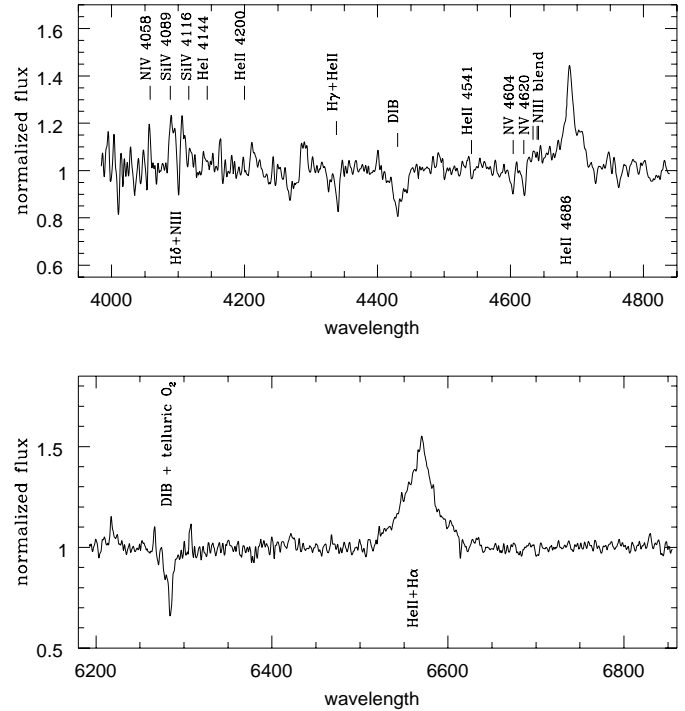


Fig. 1. Optical spectra of Wack 2134

tion, i.e. a carbon dominated WR. Hydrogen is marginally seen in late types of nitrogen dominated WR stars (WN) but is normal in O-type stars (Conti & Massey 1989).

- The emission seen in the He II $\lambda 4686$ line and N III blend $\lambda 4634$ –40–42 implies, in the case of an O-type companion, a very luminous star, that is, a supergiant. By definition, the O-type luminosity class V spectra have strong He II $\lambda 4686$ absorption. This combination of He II and N III in emission is denoted by an *f* following the spectral type (Mathys 1988; Walborn & Fitzpatrick 1990). In WN stars these lines always appear in emission.
- N IV $\lambda 4058$ emission is stronger than N III $\lambda 4640$, which is a characteristic of O3–O4 spectra. When this situation occurs an *** following the *f*, that is, *f** is used (Walborn & Fitzpatrick 1990). WN4–5 WR stars also show strong N IV $\lambda 4058$ emission (Conti et al. 1990).
- If there is an O-type star, the absence of He I $\lambda 4471$ also indicates spectral type O3–O4 (Mathys 1988; Walborn & Fitzpatrick 1990).

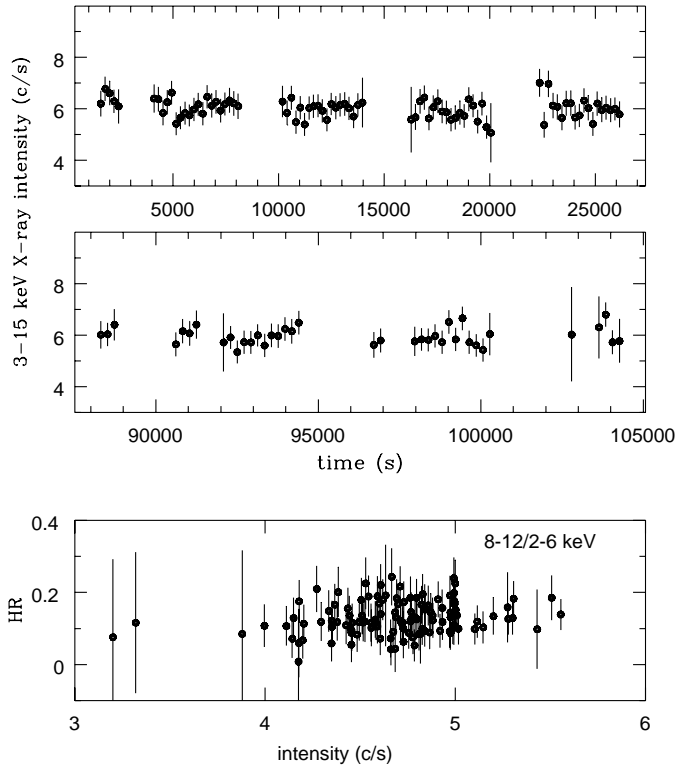


Fig. 2. RXTE PCA lightcurve of the entire observation. Also shown the HR 8–12/2–6 keV as a function of intensity. Time 0 is JD 2,450,781 at 11:26:16 and the bin size 210 s

- The lines of N V $\lambda 4604$ and $\lambda 4620$ are strongly in absorption. In WN stars these lines appear in emission or very weakly in absorption. Therefore these two lines support an O classification.
- $EW(\text{He II } \lambda 4686) \approx -6.8 \text{ \AA}$ and $FWHM(\text{He II } \lambda 4686) \approx 20 \text{ \AA}$. The value of the EW is too high for an O-type star but would agree with a WN9–11 star (Crowther & Bohannan 1997), i.e. later than the classification implied from the emission of N IV $\lambda 4058$. The FWHM is too high for both type of stars but closer to a WN star than to an O-type star.

As it can be seen the spectral classification of Wack 2134 is complex. The nitrogen lines (absorption in N V $\lambda 4604$ and $\lambda 4620$; emission in N IV $\lambda 4058$) and the presence of hydrogen seem to favour an O classification. In fact, the optical spectrum of Wack 2134 is reminiscent of HD 93129A, which is classified as O3If* (Walborn & Fitzpatrick 1990). On the other hand, the very broad, high-intensity He II $\lambda 4686$ emission would imply a WN component in the system. One is then tempted to suggest that both type of stars are present in Wack 2134, forming an early-type binary.

3.2. X-ray data

Fig. 2 shows the 3–15 keV PCA lightcurve of the entire observation. The source remained fairly constant at a mean net count rate of 6.5 PCA counts per second. Also shown in Fig. 2 is the

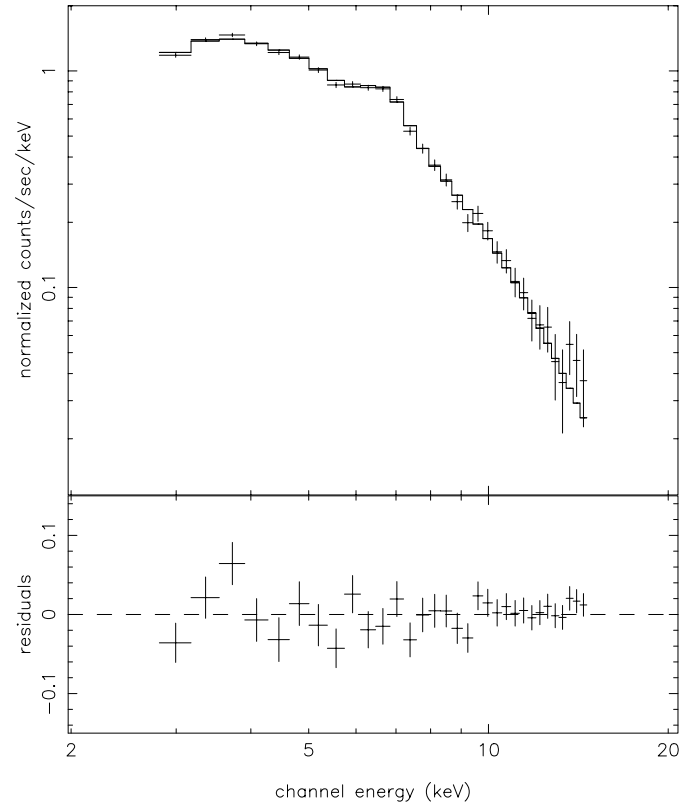


Fig. 3. X-ray spectrum of 1E 1024.0–5732 in the energy range 3–15 keV. The straight line represents the bremsstrahlung model fit plus a Gaussian component, representing an iron line at 6.6 keV

hardness ratio (HR) 8–12/2–6 keV as a function of the summed intensity in the two energy bands. Clearly, the source is a soft emitter of X-rays. We searched for the previously reported 60.7 ms period by means of a Fourier analysis. A 3500 s continuous stretch of data was divided into 21 intervals of 8192 bins each, with a bin size of 20 ms, and the resulting power averaged together. No evidence for coherent or quasi-periodic oscillations was found. Also, a period search using epoch folding techniques was performed around the 60.7 ms period but none of the trial periods showed a high enough χ^2 which could be considered as a statistically significant detection.

In order to study the long-term X-ray variability of 1E 1024.0–5732 we converted all previously reported intensities into unabsorbed fluxes in the energy range 3–15 keV. The best-fit power-law model (see below), $N_H \approx 2.9 \times 10^{22} \text{ cm}^{-2}$ and photon index 2.8, was used. The results are summarised in Table 2. For the RXTE observation the flux of the second source is estimated to be about one order of magnitude lower in the energy range 3–15 keV, assuming the spectral model given in Sect. 2.2. These numbers reveal that the source shows variability on timescales of years and a gradual increase of the X-ray flux since its discovery in 1979.

The 3–15 keV PCA RXTE spectrum of 1E 1024.0–5732 is shown in Fig. 3, where significant emission above 5 keV can be seen. The spectrum is dominated by the emission feature(s) at about 6.6 keV. Unlike X-ray pulsars, whose continuum spectral

Table 2. Long-term X-ray variability of 1E 1024.0–5732. The intensities from the different instruments were converted into unabsorbed fluxes in the range 3–15 keV by using a power-law model with $N_H=2.9 \times 10^{22} \text{ cm}^{-2}$ and $\alpha=2.8$. The assumed distance is 3 kpc.

Date of observation	Mission & Instrument	Intensity (count s ⁻¹)	Flux (10 ⁻¹² erg cm ⁻² s ⁻¹)	L _x (erg s ⁻¹)	Reference
July 13, 1979	<i>Einstein</i> IPC	0.036	2.9	3.1×10^{33}	Caraveo et al. 1989
July 8, 1980	<i>Einstein</i> IPC	0.0592	4.8	5.1×10^{33}	Caraveo et al. 1989
July 29, 1992	ROSAT PSPC	0.0756	12.6	1.3×10^{34}	Mereghetti et al. 1994
Nov 29, 1997	RXTE PCA	6.5	15.4	1.6×10^{34}	This work

shape is generally represented by a power-law with an exponential cut-off at high energies (15–20 keV), coupled with low energy absorption and, if necessary, an iron emission line at ≈ 6.4 keV, there is not such a general model to account for the X-ray spectra in colliding wind systems. A two-temperature optically thin plasma with fixed and variable solar element abundances (MEKAL and VMEKAL in XSPEC terminology) was used by Skinner et al. (1998) and Corcoran et al. (1998) to fit the X-ray spectrum of the luminous stars HD 50896/EZ CMa and η Carinae, respectively. Williams et al. (1990) found that an absorbed power-law gave the best fit to the X-ray emission of HD 193793. The low-energy X-ray spectrum of the WC8+O9I system γ^2 Vel was studied by Willis et al. (1995), who fitted a blackbody + photoelectric absorption to the observed PSPC ROSAT data and by Stevens et al. (1996), who used combinations of absorbed Raymond-Smith emission models to fit its ASCA spectrum in the energy range 0.5–5.0 keV. Thermal bremsstrahlung was considered by Williams et al. (1997) to model the production of X-ray photons from the colliding-wind Wolf-Rayet system WR147.

In order to fit the X-ray continuum we tried both, single-component models (power-law, bremsstrahlung and VMEKAL) and multi-component models (power-law plus (V)MEKAL and VMEKAL+VMEKAL). The results are summarised in Table 3. In the case of the single power-law and bremsstrahlung models an additional component (Gaussian), representing an iron line at ~ 6.6 keV was necessary to obtain small fit errors. The width of the iron line was fixed to $\sigma=0.1$ keV since it appeared to be narrower than the energy resolution of the PCA (18% at 6 keV). The line equivalent width was 470 ± 60 eV. No acceptable fit was obtained using fixed solar element abundances in the optically thin plasma model. However, the fit improved considerably when we let the Fe abundance deviate from solar, with χ^2 changing from 428 for 30 degrees of freedom (dof) to 47 for 28 dof. The best-fit temperature was achieved for $kT = 4.5 \pm 0.2$ keV. The X-ray luminosity in the energy range 3–15 keV was found to be $\sim 1.6 \times 10^{34} \text{ erg s}^{-1}$, assuming a distance of 3 kpc.

The addition of a cooler plasma component to the single temperature model with the modified Fe abundance formally improved the fit by decreasing the reduced χ^2 from 1.7 to 1.5. However, an F-test shows that the multi-component model is not statistically significant, with $\sim 30\%$ probability that the improvement in χ^2 happens by chance. Given the low S/N, low energy resolution and energy range considered (3–15 keV) it is perhaps not surprising to find difficulties in extracting reli-

Table 3. Spectral fit results. Uncertainties are given at 90% confidence for one parameter of interest. All fits correspond to the energy range 3–15 keV. An absorbed bremsstrahlung component with $N_H=2 \times 10^{22} \text{ cm}^{-2}$ and $kT = 0.5$ keV was added to all the fits (see text)

Parameter	Value
Power-law	
α	2.8 ± 0.1
N_H ($10^{22} \text{ atoms cm}^{-2}$)	$2.9_{1.1}^{2.8}$
$E_l(\text{Fe})$ (keV)	6.60 ± 0.07
$\sigma(\text{Fe})$ (keV)	0.1 (fixed)
$\chi_r^2(\text{dof})$	0.94(26)
VMEKAL	
kT (keV)	4.8 ± 0.3
Fe (\times solar)	0.35 ± 0.04
$\log(EM)$ (cm^{-3})	57.28 ± 0.09
$\chi_r^2(\text{dof})$	1.68(28)
Bremsstrahlung	
kT_{brem} (keV)	5.2 ± 0.3
$E_l(\text{Fe})$ (keV)	6.59 ± 0.07
$\sigma(\text{Fe})$ (keV)	0.1 (fixed)
$\chi_r^2(\text{dof})$	1.06(28)
MEKAL+ power-law	
N_H ($10^{22} \text{ atoms cm}^{-2}$)	~ 7
kT (keV)	$2.3_{0.5}^{0.7}$
α	2.33 ± 0.05
$\chi_r^2(\text{dof})$	1.07(27)

able abundances and deriving cooler components. In contrast, a power-law plus MEKAL with fixed solar abundances gave a good fit ($\chi_r^2=1.07$).

4. Discussion

Two models are presently competing to explain the nature of the X-ray source 1E 1024.0–5732. Both of them require the source to be a binary system. Caraveo et al. (1989) suggested that the system consists of a neutron star orbiting and early-type O star (hereafter HMXB model). On the other hand, Mereghetti et al. (1994) proposed an early-type binary system, in which the primary is a Wolf-Rayet star and the secondary an O-type star (CWB model). In the former model the X-ray radiation is due to accretion of matter onto the compact companion via a strong

stellar wind, whereas in the latter model is a consequence of colliding winds.

4.1. Optical data

From the point of view of theory the separation between O-type and WR stars does not represent a problem: O stars are assumed to be core hydrogen burning objects while WR have helium burning cores with very little hydrogen in their atmospheres. This is because WR stars are believed to be the endpoints of evolution of the most massive stars. Therefore WR stars are expected to be less massive than O-type stars. However, the distinction between these two type of stars from the point of view of the observations is not straightforward due to their very similar ionising spectrum, which is consequence of the subtypes having similar luminosities and temperature (Crowther & Bohannan 1997; Crowther et al. 1995).

The general criteria that have been traditionally used to separate the two classes have been based on the full width half maximum (FWHM) and equivalent width of the He II $\lambda 4686$, with Of stars showing narrower widths and lower equivalent widths than WN stars (Conti & Bohannan 1989). However, these criteria have to be applied with care since counter-examples can be found in the literature, such as ζ Pup, which is an O4If star having broader He II $\lambda 4686$ than some late-type WN stars (Crowther & Bohannan 1997). In the case of Wack 2134 the observed equivalent width and FWHM of the He II $\lambda 4686$ are closer to a WN star than to a single early O-type star.

When other lines are considered, the spectral features characteristic of an O-type star dominate over those of a WN star in the optical spectra of Wack 2134. Although the classification as a single O3-O4 supergiant with anomalous broad, strong He II $\lambda 4686$ emission may remain a possibility, it is more likely that the spectral lines shown in Fig 1 come from both type of stars. It is worth noting that, among WR+O binary systems, although the wind of the Wolf-Rayet companion has considerably more momentum, the O star is the more massive and likely the more luminous. Therefore it is not surprising to find a O-type like spectrum somehow distorted due to the presence of the WR component. If this interpretation is correct, it would favour the suggestion by Mereghetti et al. (1994) that the system is a colliding wind binary.

4.2. X-ray data

In Table 2 a long-term increase in the X-ray flux of 1E 1024.0–5732 is apparent. If the system is a long period colliding wind binary, then colliding wind theory (Stevens et al. 1992) would suggest that the X-ray luminosity is related to the separation D between the two components, reaching a maximum at periastron, that is, $L_x \propto D^{-1}$. Thus, a long-term increase of the X-ray flux may indicate that the system is moving towards periastron. Such behaviour has been observed in HD193793, a $P_{orb}=7.94$ yr colliding wind system (Williams et al. 1990). In support of this idea there is the fact that the flux in 1E 1024.0–5732 peaks at ~ 4 keV (Fig. 3). The theory predicts a hardening of the X-ray

emission at periastron due to the greater absorption, with the flux maximum moving from 1.5–2 keV at apastron to around 5 keV at periastron (Stevens et al. 1992). X-rays from colliding winds are expected to show up at energies ≥ 3 –4 keV, since at lower energies the soft emission from the intrinsic wind shocks of the individual components may dominate the spectrum.

The absence of X-ray emission above ~ 5 keV was considered by Skinner et al., (1998) as a proof to disregard the presence of a compact companion in the Wolf-Rayet system HD 50896 (EZ CMA). However, the opposite statement, i.e., the presence of significant X-ray emission above 5 keV, does not exclude the CWB model since theoretical models and hydrodynamic simulations of colliding wind systems predict certain level of hard (2–10 keV) X-ray emission. The hardest X-rays are expected to come from the line of centres of the system, where the highest temperature gas lies (Stevens et al. 1992; Willis et al. 1995). The X-ray emission of 1E 1024.0–5732 appears to be too soft for a HMXB. The X-ray flux decreases considerably above 15 keV, unlike other accreting pulsars also observed with RXTE which shows significant emission up to 30 keV.

Likewise, the X-ray luminosity in the energy range 3–15 keV is also lower, by about one order of magnitude, than the typical luminosity of the faintest HMXB. Table 4 shows a comparison of some observational characteristics of 1E 1024.0–5732/Wack 2134 to other CWB and HMXB with supergiant primaries. The luminosity derived from our RXTE data, $\sim 1.6 \times 10^{34}$ erg s $^{-1}$, at 3 kpc, would make 1E 1024.0–5732 one of the more luminous colliding wind systems, only comparable to HD 193793 (see Table 4). It should be noted, however, that the distance is poorly constraint and the value of 3 kpc may be considered as an upper limit (Caraveo et al. 1989). Thus, a lower X-ray luminosity is possible, which would agree with the X-ray luminosity normally seen in CWB (about one order of magnitude lower). Note also that the X-ray luminosity reported in this work corresponds to a broader energy range (3–15 keV) than normally quoted for colliding wind systems.

Single and multi-components models were used to fit the X-ray spectrum of 1E 1024.0–5732 in the energy range 3–15 keV. The results of the spectral fitting are summarised in Table 3. In the case of the optical thin plasma emission model (VMEKAL) no good fit was achieved by fixing all the element abundances to solar values, possibly indicating that the system does not consist of only an OB massive star. By letting the Fe abundance be a free parameter the reduced χ^2 decreased to acceptable levels (< 2), although it is still higher ($\chi_r^2 = 1.7$) than the other models considered. In WR stars the outer hydrogen envelope has been stripped away due to the large mass-loss rates. Therefore, WR stars are expected to be nonsolar in their chemical composition.

The fit to the overall spectrum of CWB is generally improved by using two temperature components. A cooler (< 0.7 keV) and a hotter (≥ 2 keV) components were proven to give good fits (Skinner et al. 1998; Corcoran et al. 1998). We tried the same approach here but the VMEKAL+VMEKAL model did not turn out to be statistically significant when compared to the nonsolar single temperature model. It is likely that this lack of significance is due to the conditions of our observation rather than to

Table 4. 1E 1024.0–5732/Wack 2134 compared to other colliding wind and supergiant X-ray binaries. *NS* stands for Neutron Star

Source name	Spectral Type	P_{orb} (days)	distance (kpc)	Energy range (keV)	L_x^{max} erg s $^{-1}$	Fe line (keV)	EW(Fe) (keV)	Ref.
Wack 2134	WN5-6+O3f?	-	3	3–15	1.3×10^{34}	6.60	0.47 ± 0.06	1
HD193793	WC7+O4-5V	2900	1.3	0.5–4	4.0×10^{34}	6.66	0.46 ± 0.05	2,7
V444 Cyg	WN5+O6	4.2	1.7	0.5–4	7.7×10^{32}	-	-	2
γ^2 Vel	WC8+O9I	78.5	0.45	0.5–10	4.3×10^{32}	6.9	-	3
HD 50896	WN5+?	-	1.8	0.5–10	7.0×10^{32}	-	-	4
2S 0114+650	B1Ia+NS	11.59	7.2	2–10	3.5×10^{35}	6.4	0.07–0.34	5,8
4U 1700–37	O7f+NS	3.41	1.8	1–20	3.0×10^{35}	6.47	0.07–0.40	6
Vela X–1	B0.5Ib+NS	8.96	2.0	2–30	5.0×10^{36}	6.42	0.07–0.15	9
GX 301–2	B1Ia+NS	41.5	1.8	0.7–10	1.0×10^{37}	6.40	0.228 ± 0.018	10

1: This work

2: Pollock (1987)

3: Stevens et al. (1996)

4: Skinner et al. (1998)

5: Reig et al. (1996)

6: Haberl & Day (1992)

7: Koyama et al. (1994)

8: Yamauchi et al. (1990)

9: Nagase et al. (1986)

10: Saraswat et al. (1996)

the model itself. The impossibility of RXTE to detect photons below 2.5 keV makes it difficult to constrain the temperature of a possible cooler component and the photoelectric absorbing columns. Likewise the low S/N and low energy resolution prevent us from extracting element abundances. Nevertheless, the best-fit temperatures of the bremsstrahlung and VMEKAL models, $kT \approx 5$ keV, lie in between the temperature of the hotter components in other CWB – 1.4 keV for γ^2 Velorum (Stevens et al. 1996), 3.1 keV for HD 50896 (Skinner et al. 1998) and 5.9 keV for η Carinae (Corcoran et al. 1998).

On the other hand, the good fit found with the power-law plus fixed solar abundances MEKAL model would, in principle, favour the HMXB model since, on physical grounds, we would expect thermal emission (MEKAL) from the O-type star and non-thermal emission (power-law) from accelerated electron in the accretion flow. However, one can argue that the best-fit temperature $kT = 2.3$ keV is too high to be originated in the wind of a single O star, for which much softer spectra ($kT < 1$ keV) have been observed (Berghöfer et al. 1996).

In HMXB the presence of the iron $K\alpha$ emission line is commonly seen, with a variety of strengths. It is ascribed to fluorescent reprocessing by less ionized iron in relatively cold circumstellar material. However, such a line is not exclusive of X-ray binaries but was reported to be present in, at least, two CWB: HD 193793 at 6.66 keV (Koyama et al. 1994) and in γ^2 Velorum at 6.9 keV (Stevens et al. 1996). In the case of 1E 1024.0–5732 the feature at 6.6 keV can be identified as $K\alpha$ emission from Fe XX–XXIII. From Table 4 we see that iron lines in CWB seem to be centred at slighter higher energies than in HMXB, which implies that the ionisation degree of iron in the wind surrounding the neutron star in supergiant HMXB is lower (Fe I–Fe XII) than in CWB ($>$ Fe XX). The iron line equivalent widths also tend to be larger in CWB. This difference in the energy of the iron line must also reflect a difference in the location and size of the region responsible for the line emission. The 6.4 keV line of supergiant HMXB is probably emitted from a region close to the neutron star while the ~ 6.6 keV line of CWB would be produced in the interface where the winds from the primary

and secondary collide, that is, a more extended, highly ionised plasma, located farther away from the two binary components. In this respect the 6.60 keV line observed in 1E 1024.0–5732 would favour the CWB model for this system but would deny it for η Carinae ($E(\text{Fe})=6.44$ keV). However, the true nature of η Carinae is as yet uncertain (Corcoran et al. 1998).

It is interesting to note the absence of a high energy cut-off in the power-law model fit, so typical of accreting X-ray pulsars. In bright sources this cut-off energy is seen at about 15–20 keV, but tend to decrease to 5–10 keV as the luminosity decreases (Reynolds et al. 1993). Thus, we would expect to see such a cut-off in the energy spectrum of 1E 1024.0–5732 if this source were an X-ray pulsar.

5. Conclusion and future work

The results from the optical and X-ray analysis presented in this work seem to favour the CWB model for 1E 1024.0–5732/Wack 2134. The presence of O-type and WR features in the optical spectra, the lack of X-ray pulsations, the low X-ray luminosity, the need for non-solar abundances, the relatively soft spectrum and the fact that the iron line is centred at ~ 6.6 keV are difficult to reconcile with the accreting binary model.

Further monitoring of the X-ray flux is required to confirm whether the system is approaching periastron. Radio observations are needed to search for non-thermal radiation. The detection of such type of emission would definitively confirm the nature of the system since CWB are expected to be emitters of such type of radiation, whereas not a single X-ray pulsar has been shown to emit non-thermal radio emission (Fender et al. 1997). Following the scheme by Conti et al. (1990) I- and K-band spectra would help to refine the spectral classification of the system, specially if a WR companion is present. Finally, high resolution X-ray spectra at low energies would allow the detection of different metallic lines (N, Si, Fe, Mg, S) expected from an optically thin plasma. In this respect XMM may provide the final key to unmask the true nature of this intriguing system.

Acknowledgements. The author is grateful to M.J. Coe, I. Negueruela and T. Belloni for their useful comments and to I. Papadakis for his help in the timing analysis of the X-ray data. I also thank the referee I. Stevens for his valuable comments, which improved the final version of this paper. The author acknowledges funding via the EU Training and Mobility Research Network Grant ERBFMRX/CP98/0195. The data reduction was partially carried out using the Southampton University node, which is founded by PPARC.

References

- Arnaud K.A., 1996, In: Jacoby G., Barnes J.(eds.) *Astronomical Data Analysis Software and Systems V*, ASP Conf. Series volume 101, p. 17
- Belloni T., Mereghetti S., 1994, *A&A* 286, 935
- Berghöfer T.W., Schmitt J.H.M.M., Cassinelli J.P., 1996, *A&AS* 118, 481
- Caraveo P.A., Bignami G.F., Goldwurm A., 1989, *ApJ* 338, 338
- Cassinelli J.P., Waldron W.L., Sanders W.T., et al., 1981, *ApJ* 250, 677
- Conti P.S., Bohannon B., 1989, In: Davidson K., Moffat A.F.J., Lamers H.J.G.L.M. (eds.) *Physics of Luminous Blue Variables*. IAU Colloq 113., Kluwer, p. 297
- Conti P.S., Massey P., Vreux J.M., 1990, *ApJ* 354, 359
- Conti P.S., Massey P., 1989, *ApJ* 337, 251
- Corcoran M.F., Petre R., Swank J.H., et al., 1998, *ApJ* 494, 381
- Crowther P.A., Bohannon B., 1997, *A&A* 317, 532
- Crowther P.A., Hillier D.J., Smith L.J., 1995, *A&A* 293, 172
- Fender R.P., Roche P., Pooley G.G., et al., 1997, *Proceedings 2nd INTEGRAL Workshop: The Transparent Universe*, ESA SP-382, 303
- Goldwurm A., Caraveo P.A., Bignami G.F., 1987, *ApJ* 322, 349
- Haberl F., Day C.S.R., 1992, *A&A* 263, 241
- Jahoda K., Swank J.H., Stark M.J., et al., 1996, In: Siegmund O.H.W., Gummin M.A. (eds.) *EUV, X-ray and Gamma-ray Instrumentation for Space Astronomy VII*, SPIE 2808, 59
- Koyama K., Maeda Y., Tsuru T., Nagase F., Skinner S.L., 1994, *PASJ* 46, L87
- Mathys G., 1988, *A&AS* 76, 427
- Mereghetti S., Belloni T., Shara M., Drissen L., 1994, *ApJ* 424, 943
- Nagase F., Hayakawa S., Sato N., Masai K., Inoue H., 1986, *PASJ* 38, 547
- Pollock A.M.T., 1987, *ApJ* 320, 283
- Reig P., Chakrabarty D., Coe M.J., et al., 1996, *A&A* 311, 879
- Reynolds A.P., Parmar A.N., White N.E., 1993, *ApJ* 414, 302
- Saraswat P., Mihara T., Kawai N., et al., 1996, *ApJ* 463, 726
- Shorridge K., Meyerdierks H., Currie M., Clayton M., 1997, *Starlink User Note* 86, 13
- Skinner S.L., Itoh M., Nagase F., 1998, *New Astronomy* 3, 37
- Stevens I.R., Blondin J.M., Pollock A.M.T. 1992, *ApJ* 386, 265
- Stevens I.R., Corcoran M.F., Willis A.J., et al., 1996, *MNRAS*, 283, 589
- Walborn N.R., Fitzpatrick E.L., 1990, *PASP* 102, 379
- Williams P.M., van der Hucht K.A., Pollock A.M.T., et al., 1990, *MNRAS* 243, 662
- Williams P.M., Dougherty S.M., Davis R.J., 1997, *MNRAS* 289, 1
- Willis A.J., Schild H., Stevens I.R., 1995, *A&A* 298,
- Yamauchi S., Asaoka I., Kawada M., Koyama K., Tawara Y., 1990, *PASJ* 42, L53